ION ACCELERATION IN INTENSE LASER FIELDS

T. Schlegel

GSI Helmholtzzentrum für Schwerionenforschung GmbH

EMMI 2008 Workshop on Plasma Physics with Intense Ion and Laser Beams, GSI 21. - 22.11.2008

Co-authors

V.Tikhonchuk
Centre Lasers Intenses et Applications
Université Bordeaux 1, France

N. Naumova and G. Mourou
Laboratoire d'Optique Appliquée, ENSTA,
Palaiseau, France

C.Labaune
Institute of Lasers and Plasmas and LULI, Ecole Polytechnique, France

I. V. Sokolov
Space Physics Research Laboratory, University of Michigan, USA

Outline

- Ion acceleration with high-intensity lasers: conditions and required characteristics
- Ion acceleration by the radiation pressure: the laser piston model
- Numerical simulations of the high-intensity ion acceleration and hole boring
- Effect of the electron radiation losses on the ion acceleration
- Fast Ignition with 'in situ' accelerated deuterons

Ion acceleration with intense laser pulses

Fast ions can find many applications in fusion, industry and medicine: low ratio current/ energy flux, simple ballistic transport, high absorption efficiency $\rho l \cong 10^{-3} \varepsilon_{\mathrm{i,MeV}}^{1.8}\ \mathrm{g/cm^2}$

but one needs an efficient and compact ion accelerator to energies > 100 MeV.

Two mechanisms of laser ion acceleration have been considered:

- **TNSA - target normal sheath acceleration: requires an efficient production of high-energy electrons, high-quality target surface, less restrictions on the laser pulse**

- **Ponderomotive acceleration: requires cold electrons, high-quality laser pulse, less restrictions on the target, could be more efficient**

Ion acceleration by high-energy electrons

A cloud of high energy electrons creates an electrostatic field on the density gradient and accelerates ions from the target surface: the TNSA mechanism – broad energy spectrum, Coulomb repulsion of the accelerated bunch.

Cold electrons are necessary for charge neutralization of the dense ion bunch

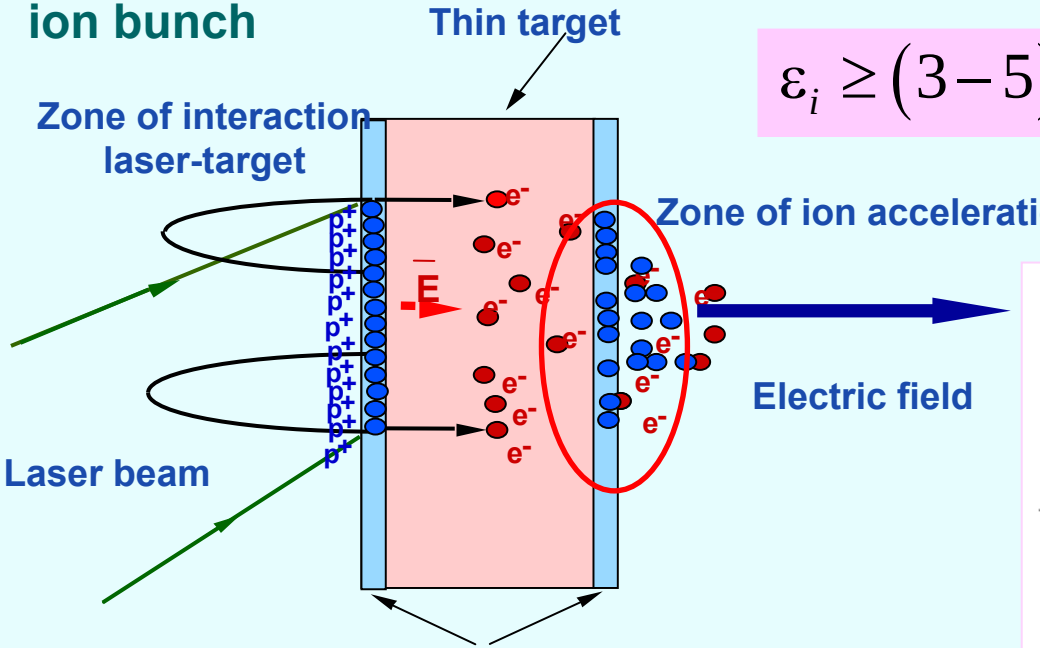

$$\varepsilon_i \geq (3-5)T_h \qquad E_a = \sqrt{n_h T_h / \varepsilon_0}$$

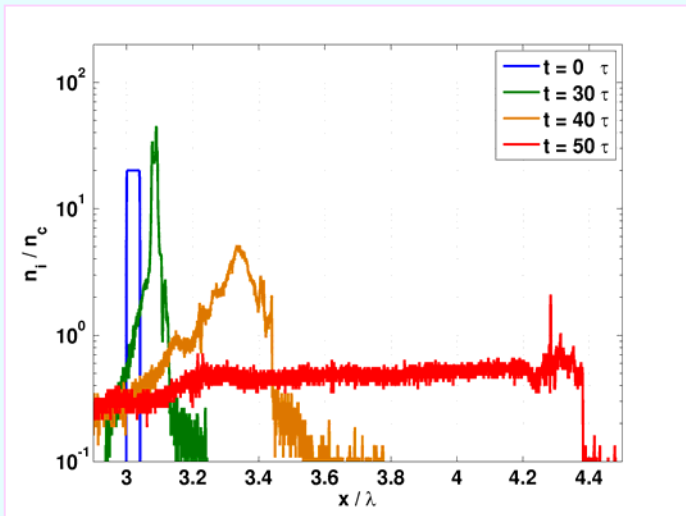

O.Klimo et al, PRST-AB, 2008

$$T_h \cong m_e c^2 \left(\sqrt{1 + 0.75\, I_{18}\, \lambda^2_{\mu m}} - 1 \right)$$

Circular *vs* linear laser polarization

Circular laser polarization suppresses the electron heating. It provides favorable conditions for ponderomotive acceleration and ion beam neutralization. Example of electron spectra at the laser intensity 1.5×10^{20} W/cm^2 and solid density.

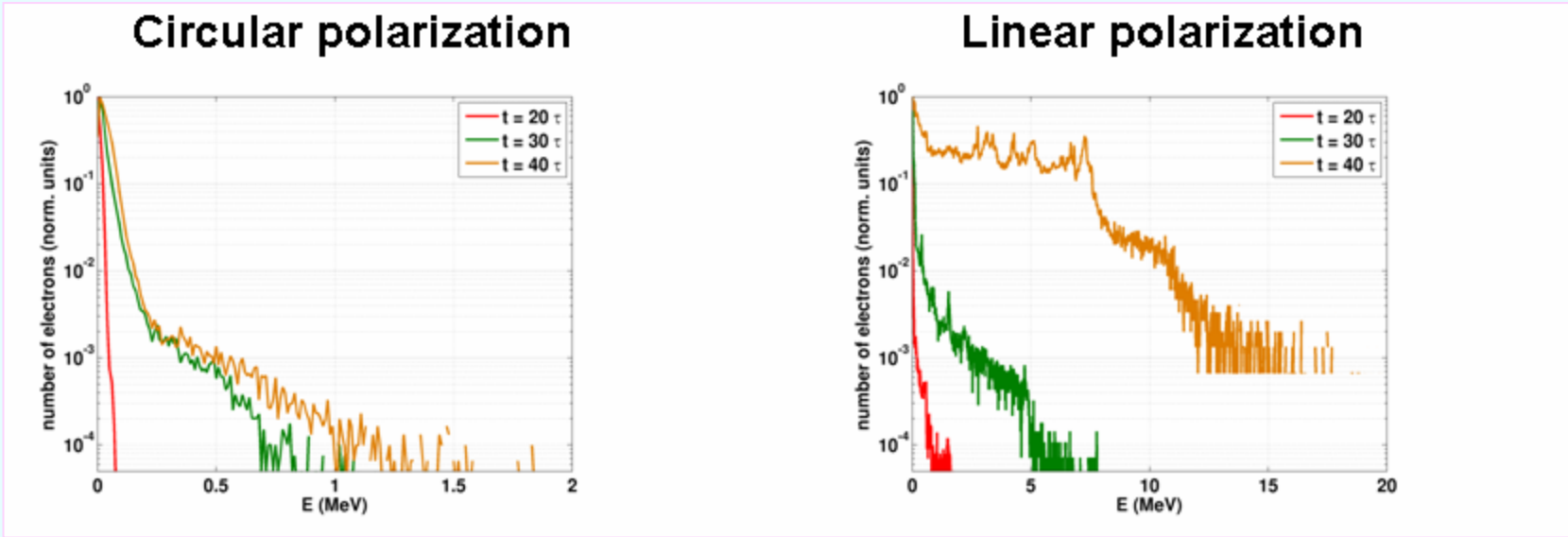

Cold electrons **Hot electrons**

O.Klimo et al, PRST-AB, 2008

Circular laser polarization and electron radiation losses are two main effects to maintain a low electron temperature

Ion acceleration by laser piston – stationary model

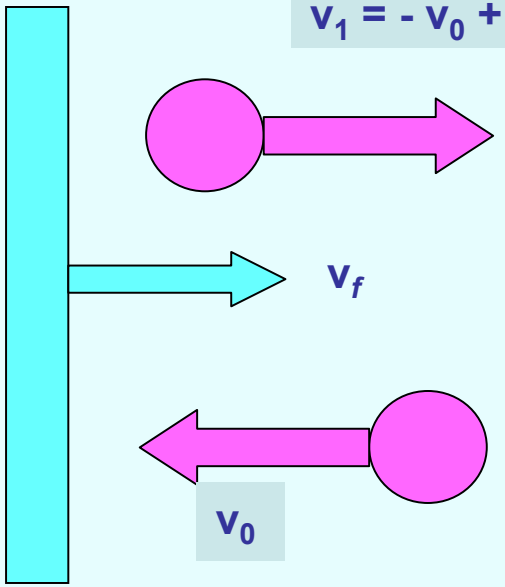

Ions are accelerated due to the elastic collisions with a moving piston

Relation between the piston and ion velocities

$$\mathrm{v}_1 = -\mathrm{v}_0 + 2\mathrm{v}_f \qquad \varepsilon_i = \tfrac{1}{2} m_i \left(2\mathrm{v}_f - \mathrm{v}_0\right)^2$$

$$p_{\mathrm{piston}} = 2 n_{0i} m_i (\mathrm{v}_0 + \mathrm{v}_f)$$

Conservation of the momentum flux (pressure) in the piston reference frame: **stationary propagation**

Ion acceleration by the laser piston: the piston velocity

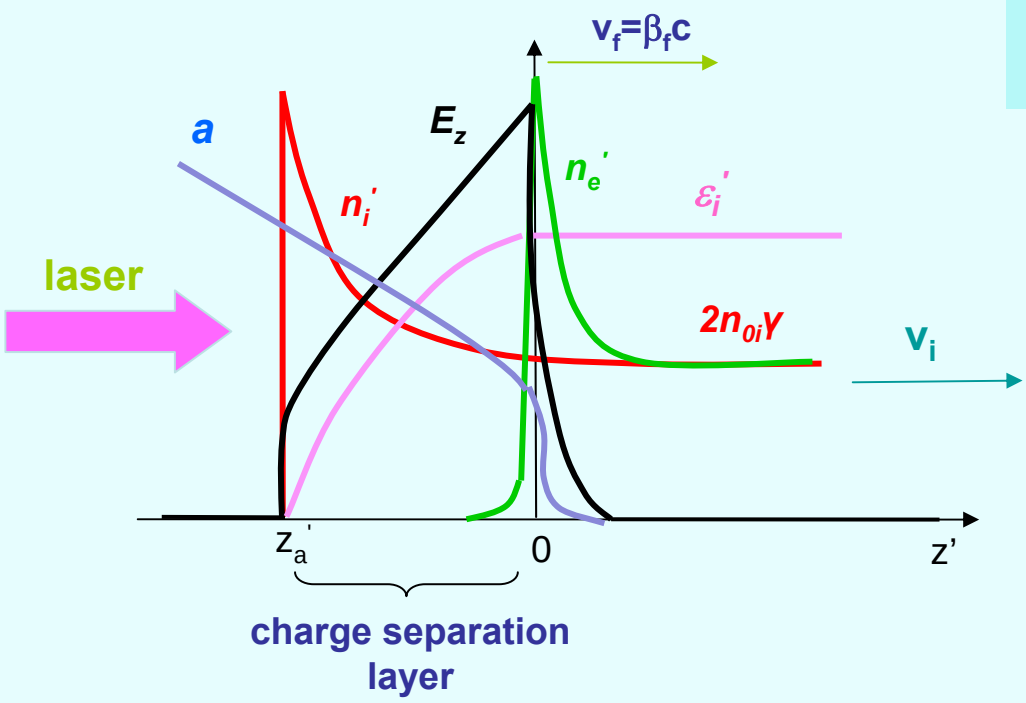

Ions are accelerated in the charge separation layer behind the electrons

Relation between the piston and ion velocities, ion energy:

$$\beta_i = \frac{2\beta_f}{1+\beta_f^2} \qquad \varepsilon_i = 2m_i c^2 \beta_f^2 \gamma_f^2$$

$$2\frac{I_{\text{inc}}}{c}\frac{1-\beta_f}{1+\beta_f} = 2n_{0i}\gamma_f\beta_f c\,(m_i + Zm_e)\gamma_f\beta_f c$$

Conservation of the momentum flux (pressure) in the piston reference frame: stationary propagation

Structure of the charge separation layer: electrostatic field and ion density distribution

The electrostatic field profile in the charge separation layer follows from the Poisson equation ($n_e = 0$)

$$\frac{d^2\Phi'}{dz'^2} = -\frac{Zen_i'}{\varepsilon_0}$$

and the ion energy and mass conservation in the piston reference frame:

$$Ze\Phi' + \varepsilon_i' = m_i c^2 \left(\gamma_f - 1\right); \qquad n_i' = 2n_{0i}\gamma_f \frac{v_f}{v_i'}$$

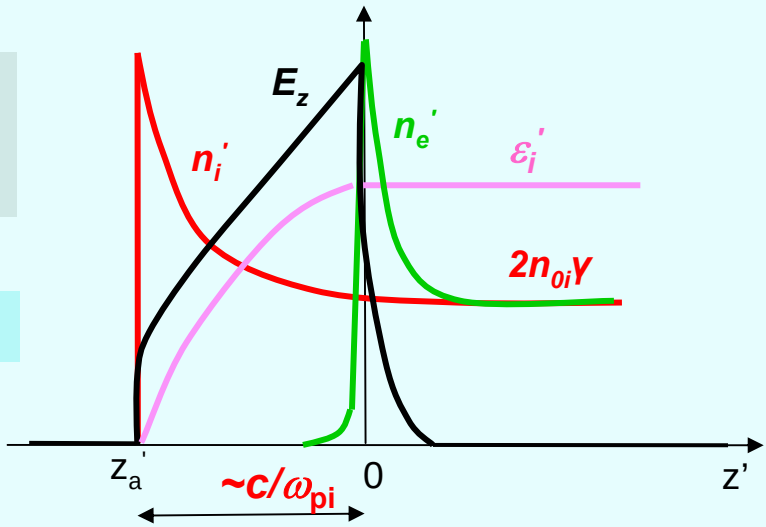

The first integral defines the electric field strength:

$$\frac{d\gamma_i'}{dz'} = 2\frac{\omega_{pi}}{c}\sqrt{\beta_f\gamma_f}\left(\gamma_i'^2 - 1\right)^{1/4}$$

$$E_z \cong \frac{2}{e} m_i \omega_{pi} c \gamma_f \beta_f$$

The layer thickness $\Delta z \sim \gamma_f c/\omega_{pi}$ for $\gamma_f >> 1$

Structure of the ion charge separation layer

a) velocity of the accelerated ions in the piston reference frame
b) ion γ-factor

c) ion density distributions
d) spatial distributions of the electrostatic potential and field

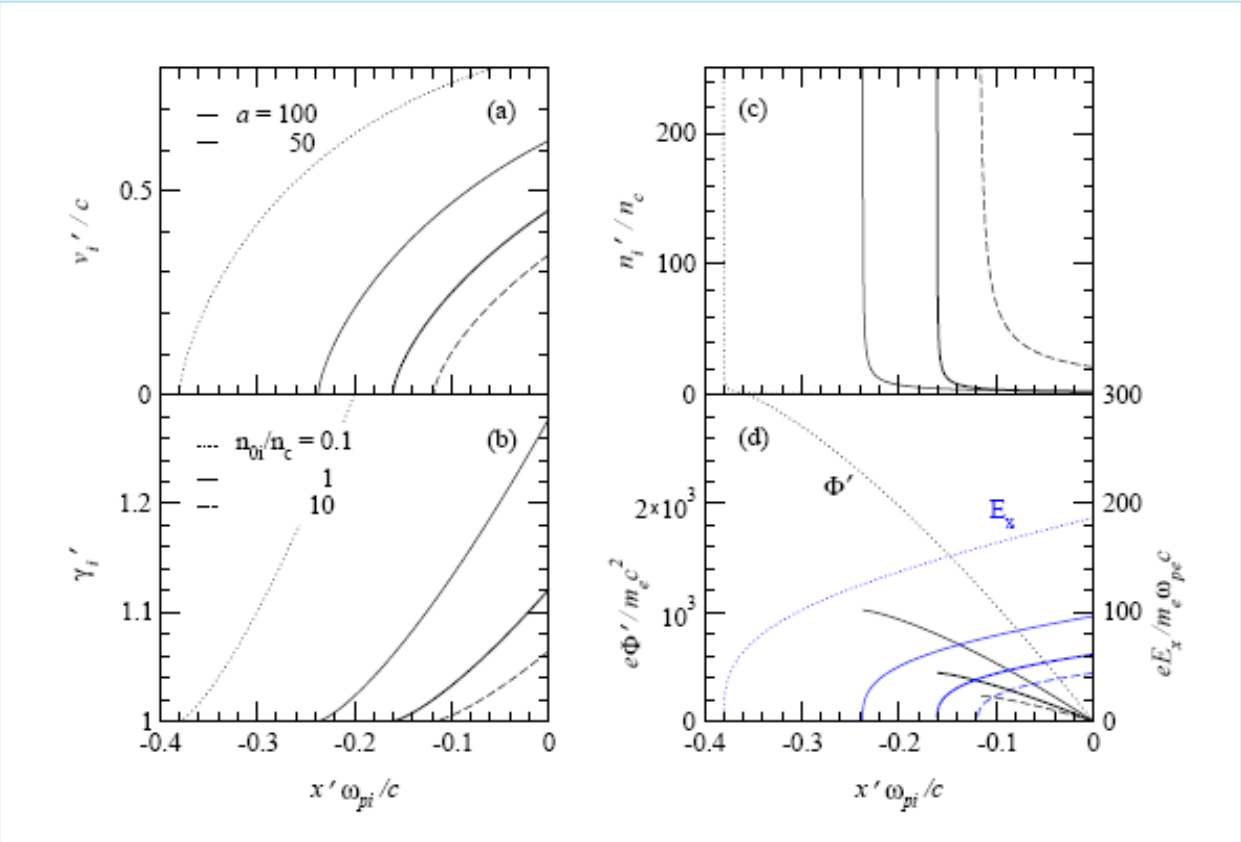

Structure of the electron sheath: laser field and electron density distribution

The electrostatic field profile in the charge separation layer follows from the Poisson equation

$$\frac{d^2\Phi'}{dz'^2} = -e\frac{Zn_i' - n_e'}{\varepsilon_0}$$

The electron energy and the laser amplitude obey the equations:

$$\frac{d^2\gamma_e'}{d\zeta^2} = 2\gamma_f\beta_f\frac{n_{0i}}{n_c}\left(\frac{Z\gamma_e'}{\sqrt{\gamma_e'^2 - 1 - a^2}} - \frac{\gamma_i'}{\sqrt{\gamma_i'^2 - 1}}\right)$$

$$\frac{d^2a}{d\zeta^2} = 2\gamma_f\frac{n_{0i}}{n_c}\frac{Z\beta_{fa}}{\sqrt{\gamma_e'^2 - 1 - a^2}} - \frac{1-\beta_f}{1+\beta_f}a$$

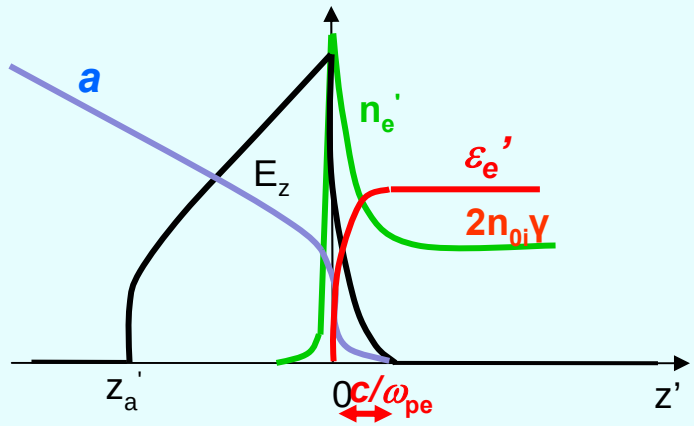

$$\zeta = z'\frac{\omega}{c}$$

The electron layer thickness c/ω_{pe}, the laser field $a_{\zeta=0} \approx \gamma_f\beta_f$

Structure of the electron sheath

a) particle velocities
b) γ-factors
c) electron and ion densities

d) vector potential
e) electrostatic potential
f) electrostatic field

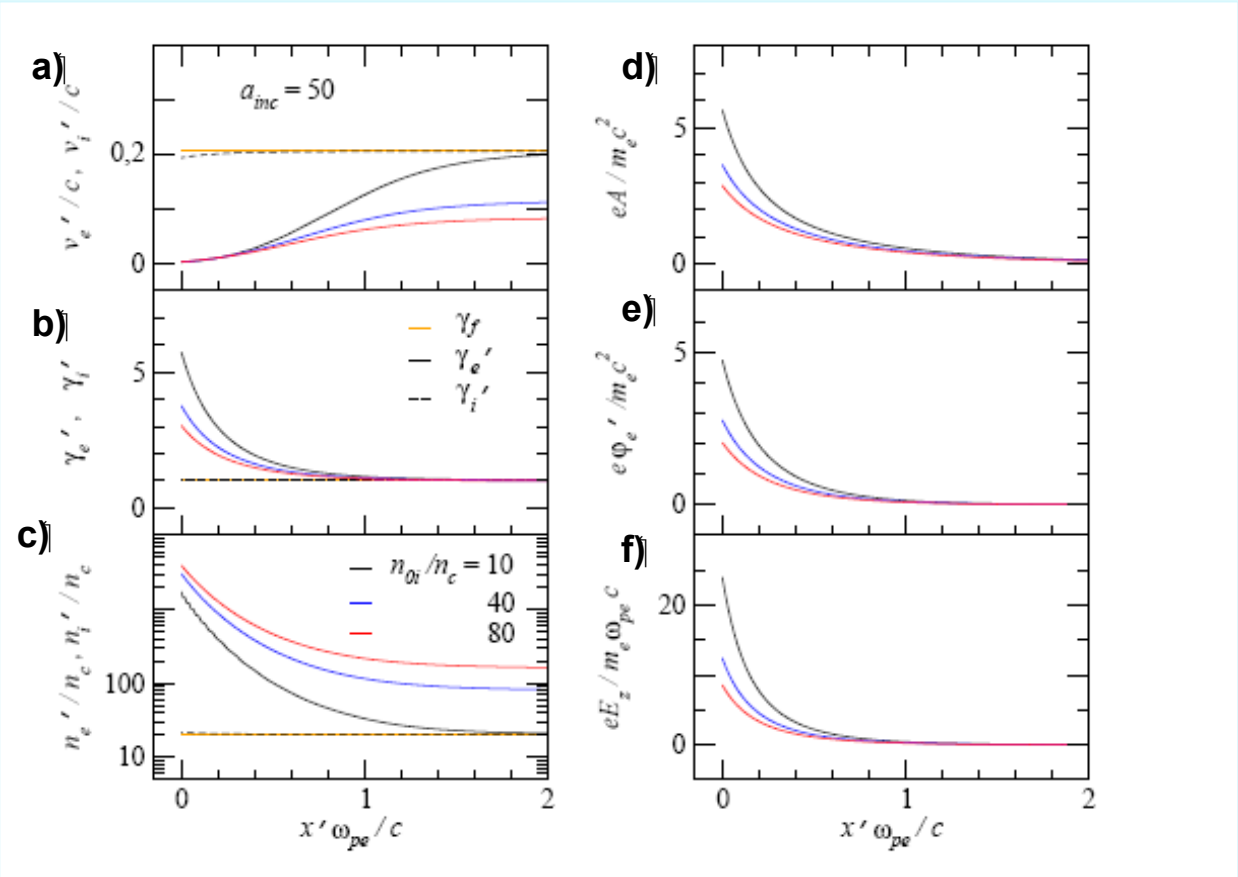

Laser potential in the electron sheath

Laser potential on the board of the electron charge separation layer a_0 is ~ 20 times larger than one would qualitatively expect $a_{\zeta=0} \approx \gamma_f \beta_f$ and it decreases slower with the plasma density

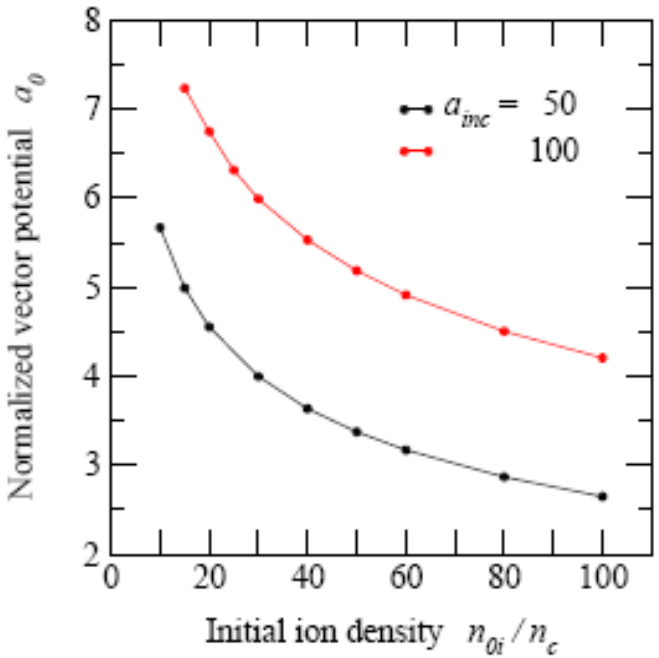

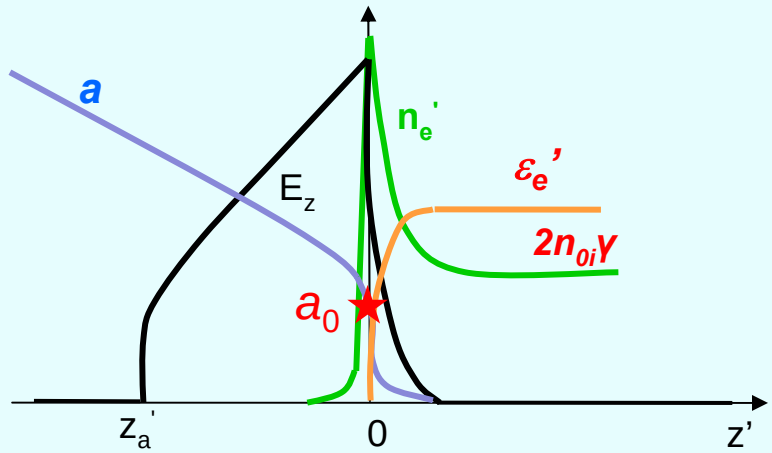

A very tight balance between the ponderomotive potential and the electrostatic field makes the electron confinement very unstable

Efficiency of ion acceleration by the laser piston

$$\beta_f = \frac{B}{1+B} \quad \text{where } B = \sqrt{\frac{I_{\text{inc}}}{n_{0i} m_i c^3}}$$

Piston velocity depends on the laser intensity and the plasma density

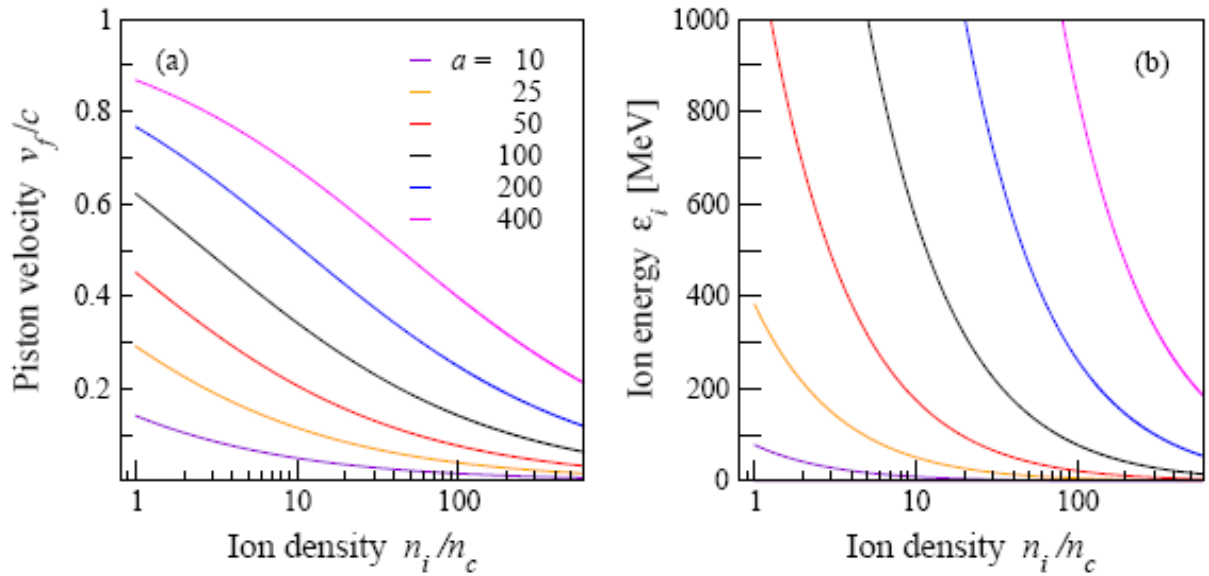

Efficiency of laser-ion energy transfer depends on the piston velocity

$$a = \sqrt{I_{\text{inc}} / n_c m_e c^3} \cong 0.61 \sqrt{I_{18}}\, \lambda_{\mu\text{m}}$$

$$\varepsilon_i = 2 m_i c^2 \beta_f^2 \gamma_f^2$$

$$1 - R = \frac{2\beta_f}{1+\beta_f}$$

Ion energy spectrum in an inhomogeneous plasma

Ions are mono-energetic in a homogeneous plasma, in an exponential density profile the ions are a power spectrum

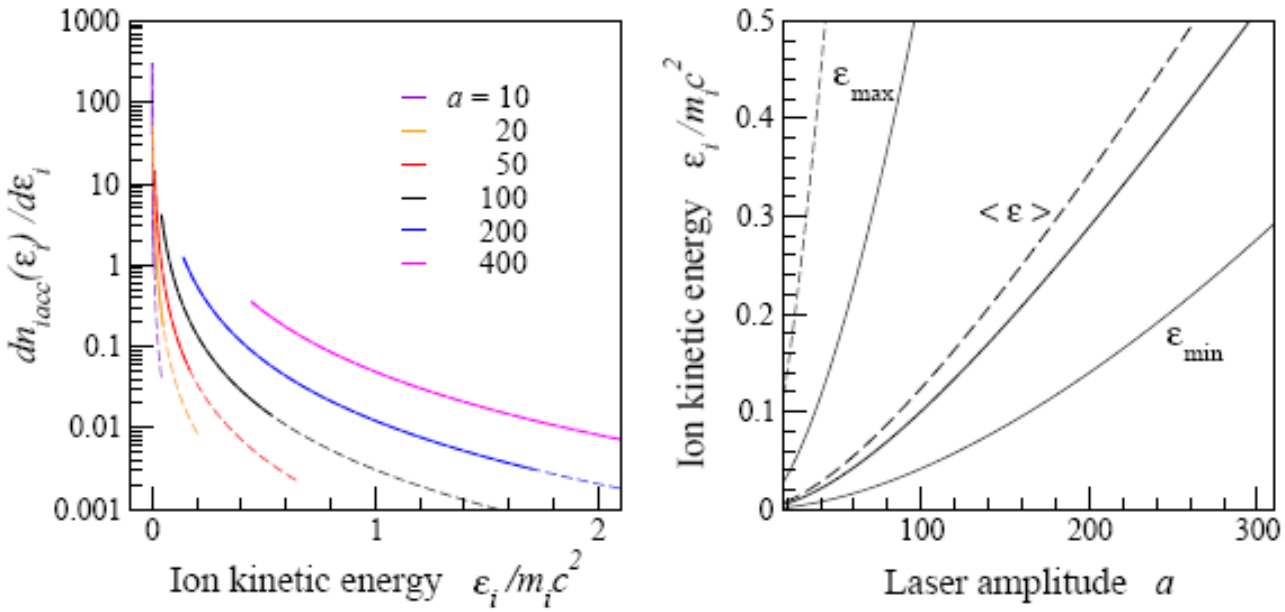

Deuteron spectra in a plasma with the density increasing from 1 to 100n_c

$$\frac{dN_i}{d\varepsilon} = \frac{I_{\text{inc}} L}{2m_i^2 c^5} \frac{1}{\beta_f^4 \gamma_f^6 \left(1+\beta_f\right)}$$

$$\left\langle \varepsilon_i \right\rangle = \frac{4I_{\text{inc}}}{n_{i\max} c} \ln \frac{\beta_{f\,\min}}{\beta_{f\,\max}}$$

Time of hole boring and laser fluence

Time of ion acceleration depends on the difference between the photon and piston velocities

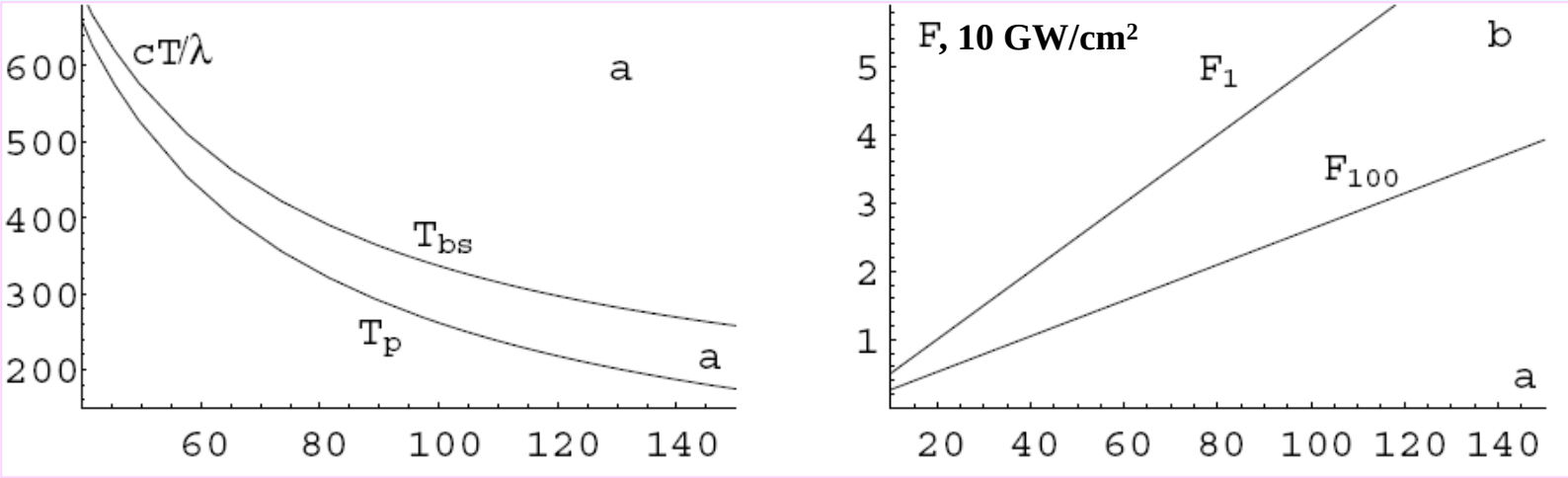

$F_{100} = I_{inc} T_p$ is the laser flux needed for accelerate ions from the density increasing from 1 to 100n_c over the length of 100λ, F_1 is the same for the density range 0.1 to 1n_c over the length of 1000λ

$$T_p = \sqrt{\frac{m_i c}{I_{\text{inc}}}} \int \frac{L \mathrm{d}n_i}{\sqrt{n_i}} \qquad F_{\text{las}} = \sqrt{m_i c I_{\text{inc}}} \int \frac{L \mathrm{d}n_i}{\sqrt{n_i}} \qquad F_i \approx \int L \varepsilon_i(n_i) \mathrm{d}n_i$$

1D & 2D PIC simulations of ion acceleration & hole boring

The code accounts for the electron radiation in the laser field and for the electron slowing down due to the radiation emission

Laser pulse:

$a_{inc} = 100$

circularly polarized

$I_{inc} = 4\times10^{22}$ W/cm^2

$\tau = 188\ \lambda/c$

2D: $d/\lambda = 20$ flat-top with expon. wings

Plasma: deuterium

exponential profile

$L_p/\lambda = 60$; $L/\lambda = 20$

$n_0/n_c = [5\text{-}100]$

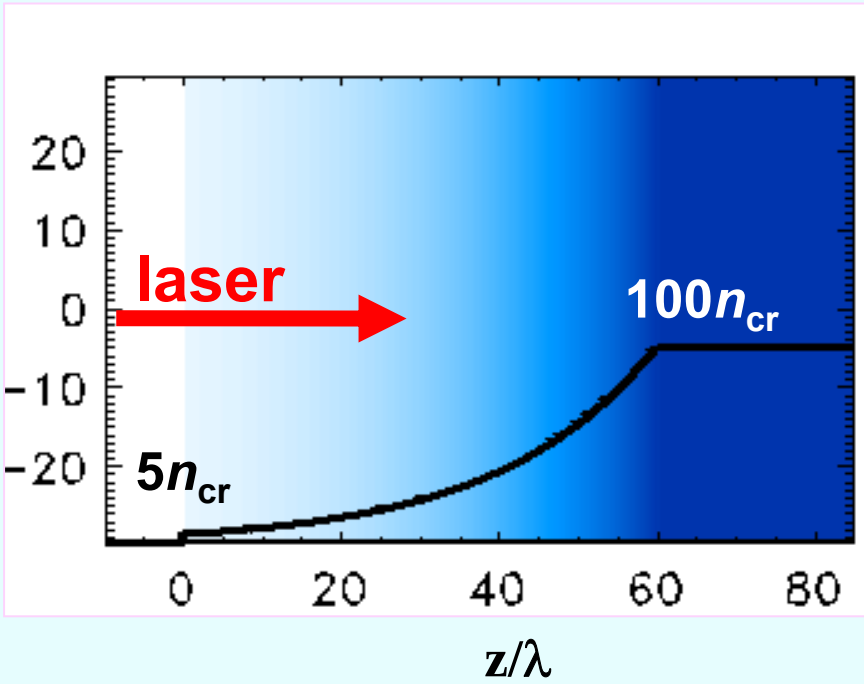

1D PIC simulation – electron & ion phase plots

$t = 30\ \lambda/c$ beginning of acceleration

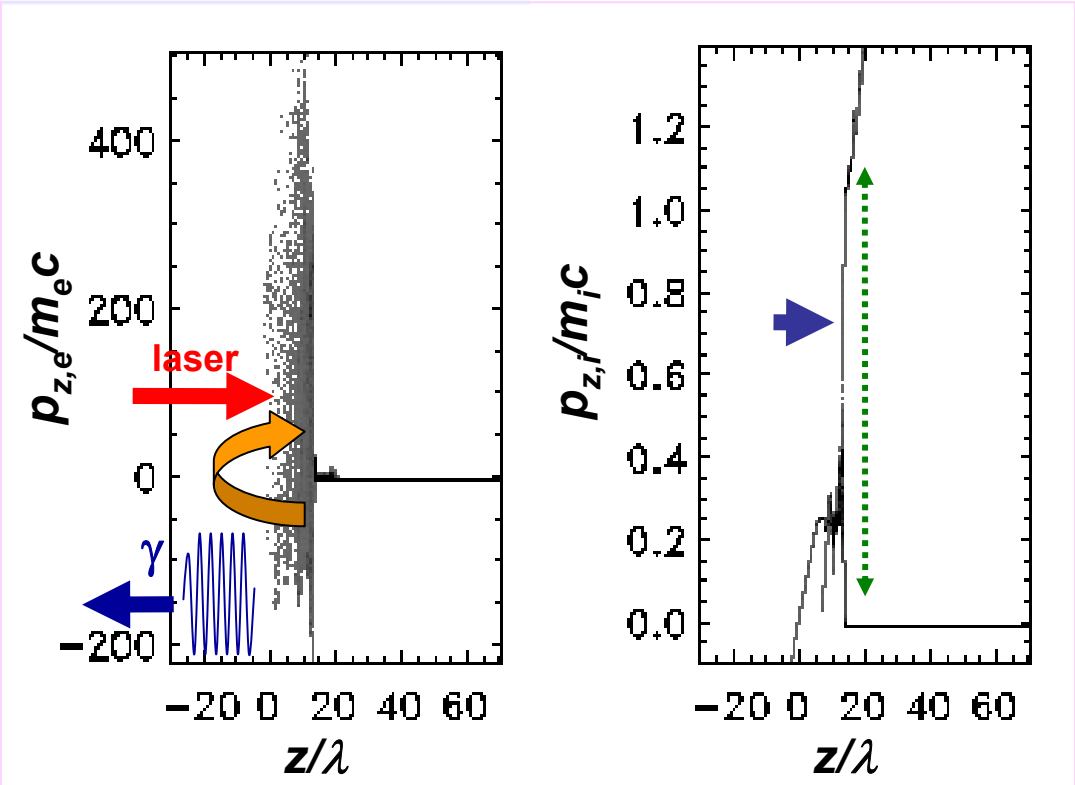

electrons ions

Electron radiation losses assure the quality of the piston

- **Electrons maintain the acceleration field: they are driven by the ponderomotive force of the laser field in the forward direction, while the charge separation field accelerates them backwards.**
- **Ions driven by the charge separation field are accelerated and move forward.**
- **Almost complete neutrality is maintained in front of the piston**
- **Some electrons escape the piston: they are losing their energy by generating high energy photons, and reverse their motion.**

1D PIC simulations with/without radiation reaction

Laser pulse: a = 100, circular polarization, t = 200T, plasma: n = 10n_c,m_i = 2m_p.

electrons

- **High quality ion beam**
- **14% of the laser pulse energy of 28 laser cycles is converted into a high frequency radiation!**

ions

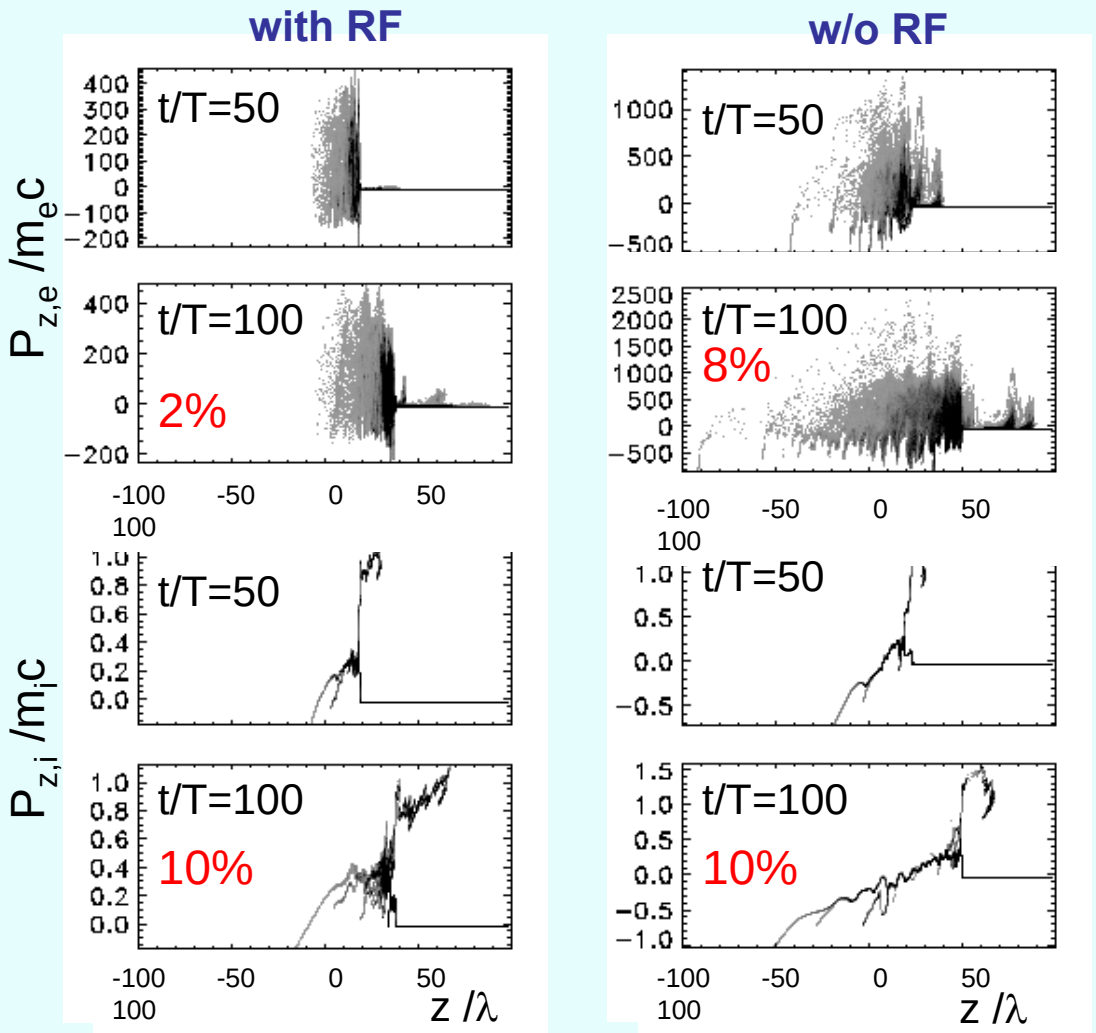

Radiation Reaction: Compton-Thomson Cooling

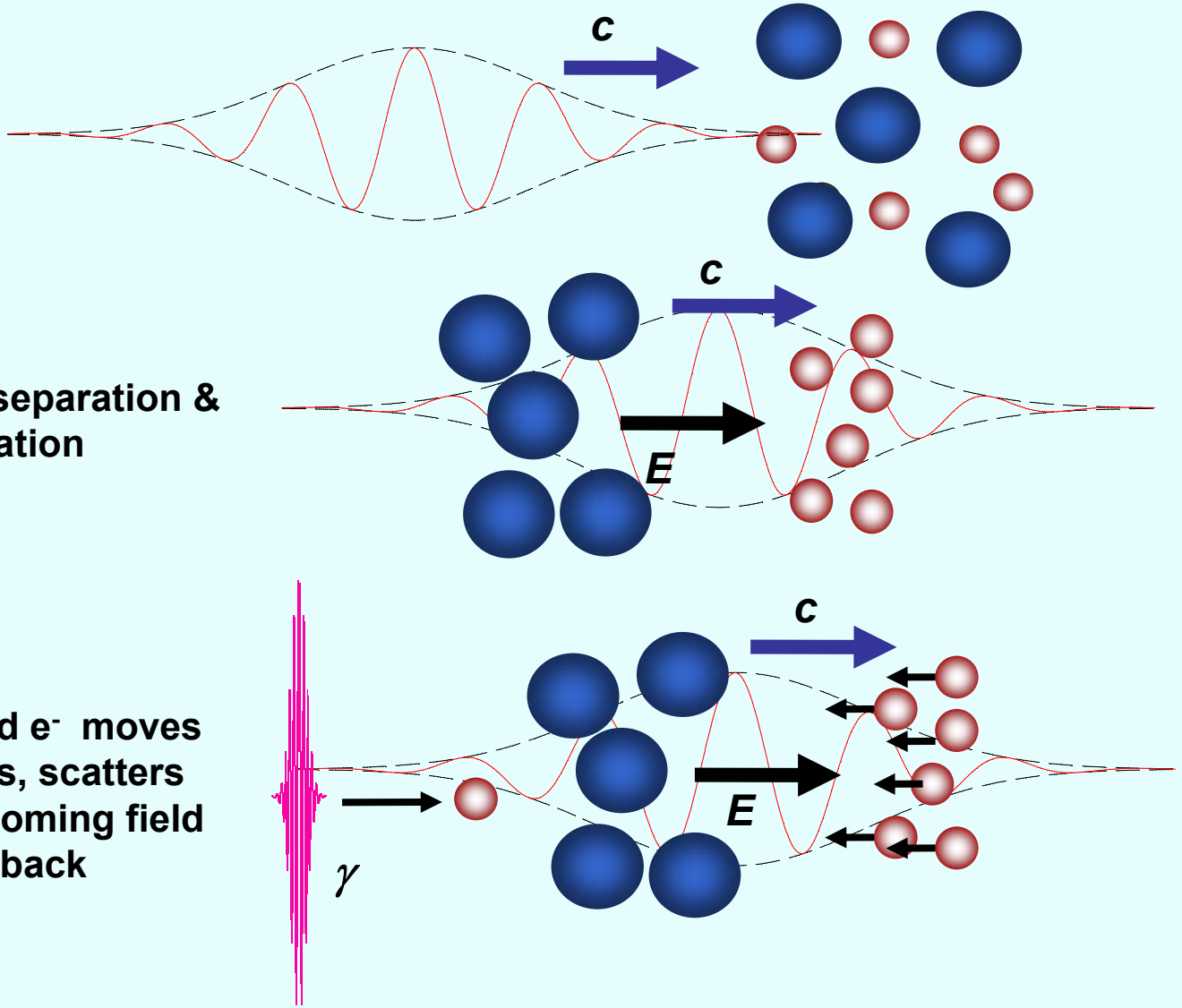

a) charge separation & E-field creation

b) escaped e^- moves backwards, scatters on the incoming field & returns back

Electron radiation slowing down

Thomson scattering is strongly amplified in the relativistic laser field due to high order harmonic generation:

$\gamma_e << a$ $\qquad\qquad$ $\gamma_e >> a$

$$N_{\max} \cong a^3, \quad P_{\rm rad} \cong \frac{e^2\omega^2}{3\pi\varepsilon_0 c} a^4 \qquad N_{\max} \cong a\gamma_e^2, \quad P_{\rm rad} \cong \frac{e^2\omega^2}{3\pi\varepsilon_0 c} a^2\gamma_e^2$$

Radiation is enhanced if the electron propagates toward the laser beam with a high energy, $\gamma_e >> a >> 1$.

The photons with the frequencies $\omega_{ph} \sim \omega\, a\, \gamma_e^2$ are emitted in a narrow cone $\theta \sim a/\gamma_e << 1$.

The electron radiation stopping length reads

$$l_{\rm rad} \cong \frac{c^2}{r_e\omega^2}\frac{1}{\gamma_e a^2} \cong \frac{1}{40}\frac{\lambda^2}{r_e a^4}\frac{n_i}{n_c} \sim 3-5\,\mu\text{m}$$

for $n_i/n_c = 40$ and $a = 100$.

1D PIC simulation – ion energy distribution

$t = 250\ \lambda/c$ end of acceleration

Laser fluence: 20 GJ/cm^2
Ions: 5.4 GJ/cm^2 (27%)
Electrons: ~1%
High energy photons: ~ 10%

The ions are gaining the main part of laser energy, the electrons remain cold due to the radiation losses

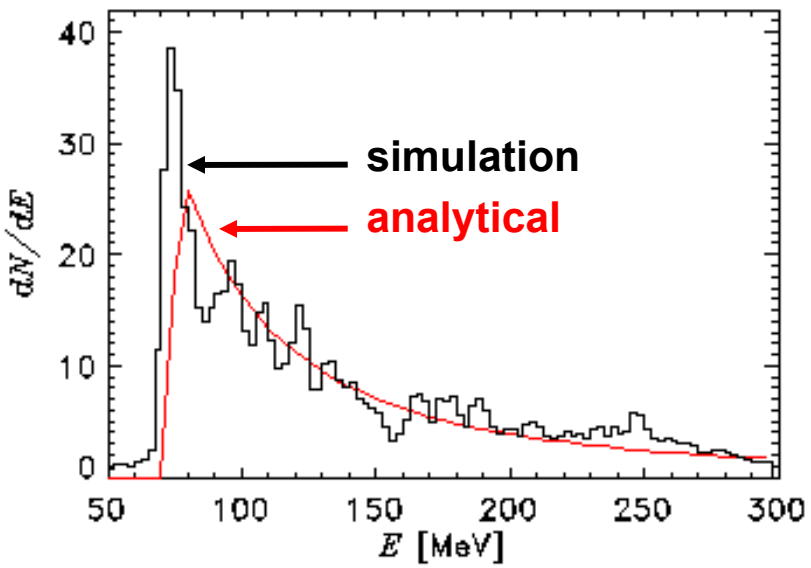

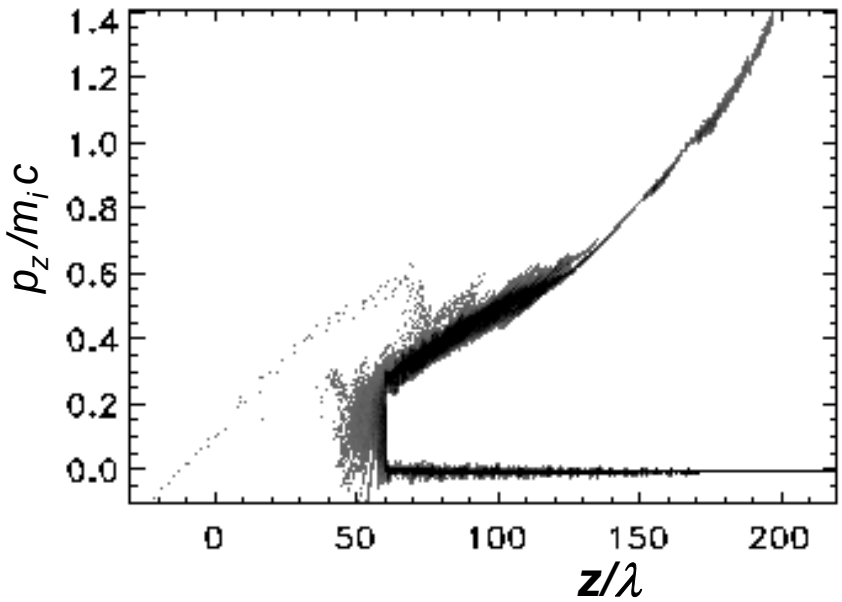

2D PIC simulation – channel formation

Flat-top laser intensity profile

Ion density distribution demonstrates efficient hole boring in the plasma, a clean and a stable channel

Filamentation is strongly suppressed due to radiation losses

Velocity of hole boring is in agreement with the 1D model

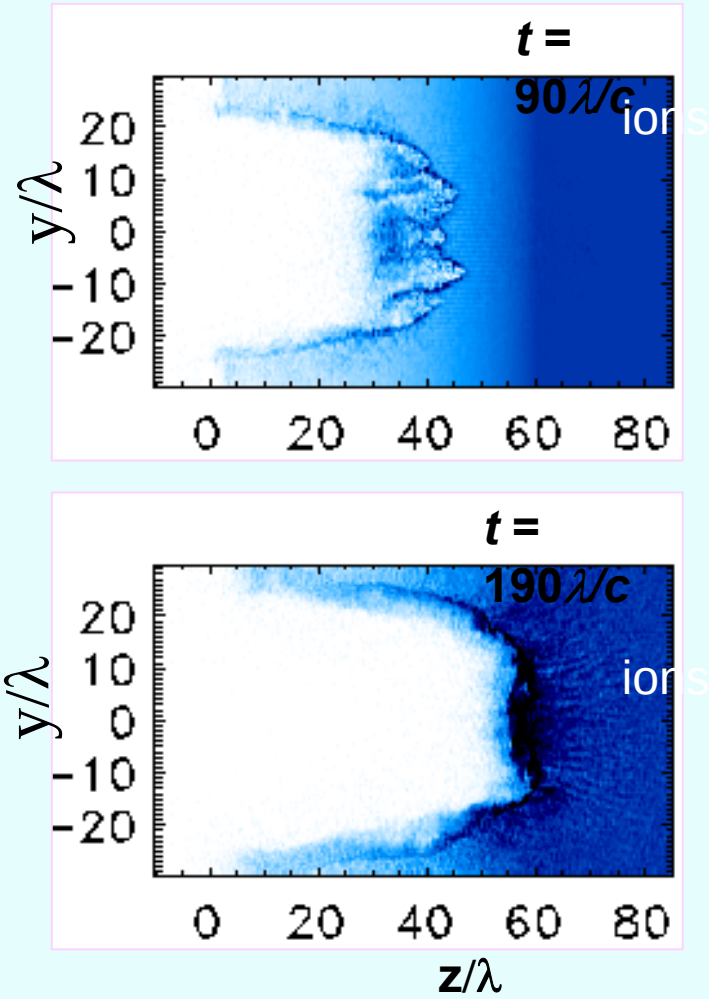

2D PIC simulation – ion energy distribution and angular spread

Angular distribution of ions *vs* energy at the final instant at $|y/\lambda| < 10$ shows a narrow peak in forward direction

Energy distribution in the central part (a cone of 6°) agrees well with 1D PIC simulations and analytical model

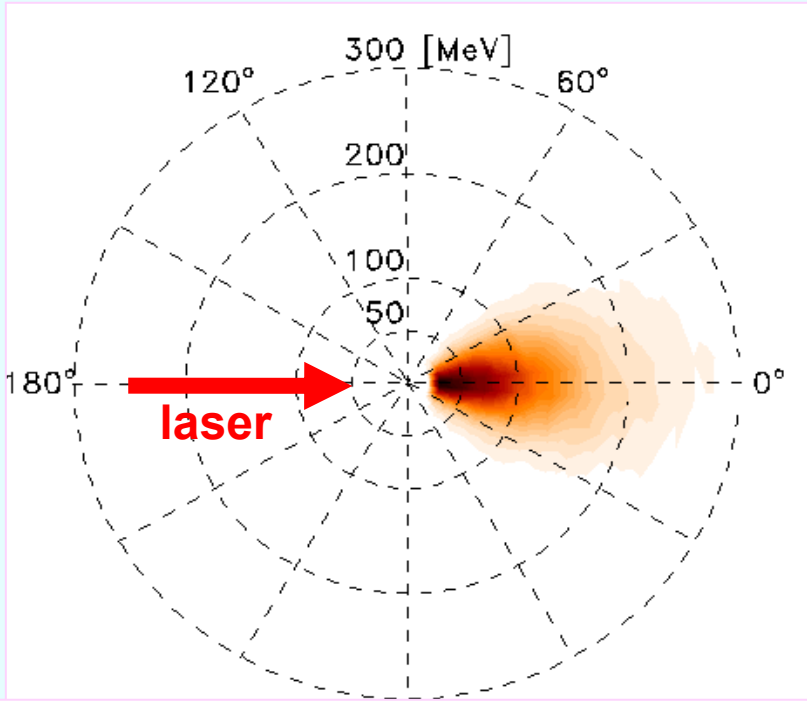

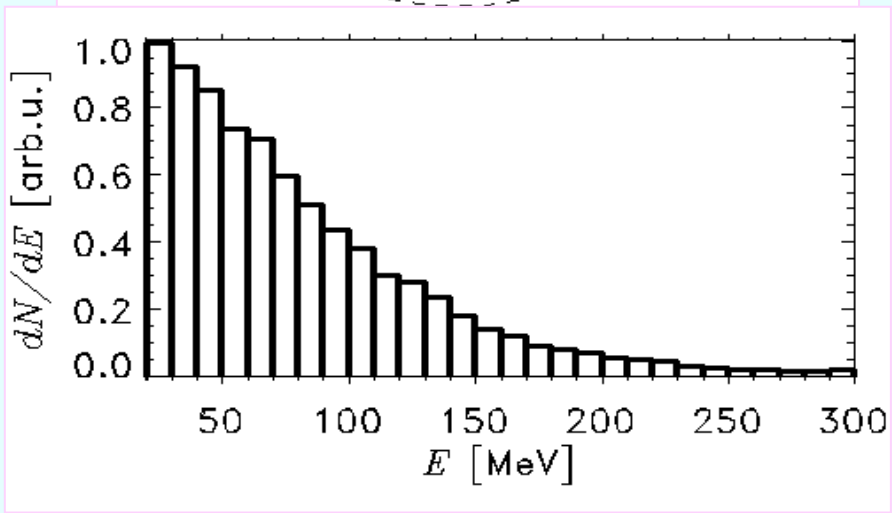

Conclusions

- Laser acceleration of ions to high energies by the ponderomotive pressure could be efficient at high intensities: high contrast and circular polarization are needed
- A model of a laser piston predicts the ion energy spectrum as function of the laser and plasma parameters. Efficient ion charge neutralization by cold electrons
- Numerical simulations are in a good agreement with the model at high plasma densities: suppression of laser beam filamentation in the channel, stabilizing effect of electron radiation losses on the channel formation
- More extended 1D & 2D simulations are under way: electron radiation losses, stability of ion acceleration, ion beam divergence